Hindawi Publishing Corporation
Journal of Electrical and Computer Engineering
Volume 2015, Article ID 782851, 9 pages
http://dx.doi.org/10.1155/2015/782851

Research Article

Analysis of an Underground Vertical Electrically Small Wire Antenna

Shuwei Dong, Aiguo Yao, and Fanhe Meng

Faculty of Engineering, China University of Geosciences, Wuhan, Hubei 430074, China

Correspondence should be addressed to Aiguo Yao; a.yao@cug.edu.cn

Received 30 November 2014; Revised 11 January 2015; Accepted 13 January 2015

Academic Editor: John N. Sahalos

The problem considered is a vertical electrically small wire antenna located underground, which transmits electromagnetic signals to the ground. Getting Green's function of the vertical dipole underground was the first step to calculate this issue. A quasistatic situation was considered to make an approximation on Sommerfeld integral for easy solution. The method of moments was used to solve the current distribution on the antenna surface at different frequencies, which laid a good foundation for obtaining the electric field of the antenna. Then the axial and radial components of the electric field with the radial distance on the ground were investigated, as well as the voltage received on the ground. Furthermore, the influence of the frequency and stratum parameters on current and electric field was studied to understand the variation clearly.

1. Introduction

Underground antenna has wide applications in many areas such as energy, geology, and military. One example is the application in measurement while drilling (MWD), an advanced technology in drilling engineering, in which the electromagnetic wave generated by an underground antenna makes a role of an information carrier from the underground to the ground. The problem of electromagnetic propagation through different media has been considered by many scholars beginning with Sommerfeld [1]. Sommerfeld treated a vertical dipole placed at the surface of ground and used the evaluation of Fourier-Bessel integrals to solve this problem. Moore and Blair [2] did an analysis on dipole radiation in a conducting half space and gave expressions of the fields in 1961. Bannister [3–5] did a series of studies about quasistatic fields of antennas at or above ground using image theory and made a conclusion of his achievements in 1979. Chang and Wait [6] made a research about extremely low frequency propagation along a horizontal wire located above or buried in the earth and derived explicit expressions for the propagation constant in 1974. King [7] did a study about a vertical dipole over an imperfectly conducting half space as early as 1990. In 1997, King et al. [8] studied a very low frequency antenna in the sea and gave the results of electromagnetic fields. In 2000 Tai and Collin [9] researched the radiation of a Hertzian dipole immersed in a dissipative medium. In 2004 Thottappillil et al. [10] gave the formulas of a semi-infinite antenna that was above a conducting plane. In 2010 Khalatpour et al. [11] presented a method for evaluation of impedance and current distribution of a vertical wire antenna above lossy ground; this work was completed by using the matrix pencil method. In 2010 Zou et al. [12] presented a fast algorithm for calculating the field excited by a vertical dipole over a lossy ground; the integrals in this work were decomposed into two parts, one could be calculated by a recursive analytical expression and the other can be calculated numerically. In 2011 M. P. Rančić and P. D. Rančić [13] proposed a new model to solve the current distribution and input impedance of a horizontal dipole antenna above a homogenous lossy half space; the method proved to be accurate and effective. In 2012 Poljak et al. [14] derived a time domain variant of the generalized telegrapher's equations for the field coupling to finite length wires above a lossy ground and gave some computational examples; this work was fully based on the problem of a thin wire antenna above a lossy medium. In 2014 Christakis et al. [15] solved the problem of radiation from a vertical short dipole antenna above lossy ground and used the stationary phase method to obtain the field formulation with closed form analytical solution in

the high frequency regime. In 2014 Pan and Li [16] introduced the solution for extremely low frequency (ELF) or super low frequency (SLF) wave propagating in different regions. In relevant chapter of their book, the scholars studied a horizontal electric dipole located on the boundary between the sea and the ocean floor and make a further study of a horizontal electric dipole in the three-layered region or n-layered region. In these studies, the formulas of the dipole and some computations are presented and discussed. However, the research on the field excited by an underground electrically small antenna is not common, and the theory of the underground antenna induction field is not mature. An electrically small antenna with ELF or SLF can be the best choice for underground electromagnetic communications generator. What is more, this kind of antenna can also play a good role in areas such as energy development, trenchless technology, mine communication, geophysical prospecting, and lateral wells butt and monitoring of underground targets.

In this paper, we proposed a model of a vertical electrically small antenna located underground with ELF or SLF. To get the expressions of the field generated by underground antenna, quasistatic approximation has been used for overcoming the calculation difficulties caused by Sommerfeld integral. Numerical results including the current distribution, electric field, and voltage received have been obtained by using the method of moments (MOM). Further study has been done to get the variation curves of the current and electric field with the frequency or stratum parameters.

2. Mathematical Procedure

For a homogenous medium, (1) which the magnetic vector potential $\mathbf{A}$ satisfied can be obtained from Maxwell's equations

$$\nabla^2\mathbf{A} + k^2\mathbf{A} = -\mu\mathbf{J}, \tag{1}$$

where $\mathbf{J}$ is the current density of an impressed source, k is the wave number given by $k^2 = -i\omega\mu(\sigma + i\omega\varepsilon)$, ε, μ, and σ are, respectively, the permittivity, permeability, and conductivity of the medium, and ω is the angular frequency. In this equation and the following analysis, the time dependence $e^{i\omega t}$ is assumed and suppressed. Solving this equation, the vector potential $\mathbf{A}$ can be determined by

$$\mathbf{A}(\mathbf{r}) = \mu\int_V G\left(\mathbf{r}-\mathbf{r}'\right)\mathbf{J}\left(\mathbf{r}'\right)\mathrm{d}V', \tag{2}$$

where G is Green's function.

Consider the ground as a homogenous conducting medium; there is a time harmonic vertical dipole buried in the soil as presented in Figure 1. The air occupies the upper half space characterized by the permittivity ε_0 and permeability μ_0 while the ground occupies the lower half space characterized by the permittivity $\varepsilon_1 = \varepsilon_r\varepsilon_0$, permeability μ_0, and conductivity σ_1. Because of the image effect, the field excited by the vertical dipole is the superposition of primary field and reflected field of the source. And in this case, Green's function underground is expressed as

$$G_1(\mathbf{r}) = G_1\left(\mathbf{r}-\mathbf{r}'\right) + G_1\left(\mathbf{r}-\mathbf{r}''\right), \tag{3}$$

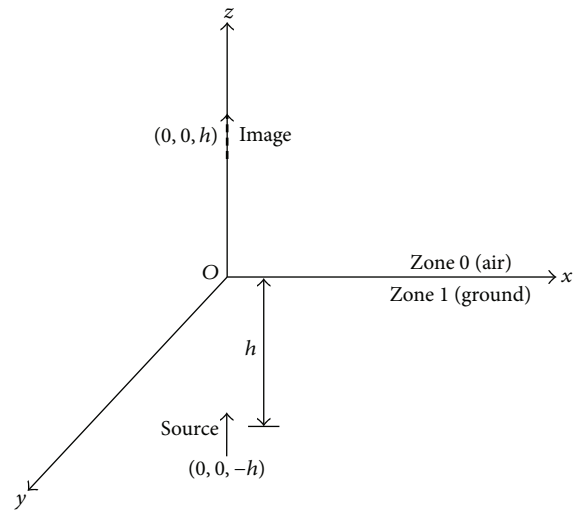

Figure 1: Schematic of the vertical dipole.

where $\mathbf{r}$ is the field point, $\mathbf{r}'$ is the source point, and $\mathbf{r}''$ is the image source point, respectively. Assume the coordinate origin is at the surface of the air and ground and the coordinates of the vertical dipole are $(0, 0, -h)$ while the coordinates of its image are $(0, 0, h)$, where $h > 0$.

According to what we have known of Green's function of the vertical dipole in the free-space, the overground Green's function of the dipole can be expressed as the following expression (4a) while the underground Green's function is shown as (4b), according to the image theory [17]

$$G_0(\mathbf{r}) = \frac{1}{4\pi}\int_0^\infty P\frac{k_\rho}{\xi_0}e^{-\xi_0|z+h|}J_0\left(k_\rho\rho\right)\mathrm{d}k_\rho, \tag{4a}$$

$$G_1(\mathbf{r}) = \frac{1}{4\pi}\int_0^\infty\left(\frac{k_\rho}{\xi_1}e^{-\xi_1|z+h|} + Q\frac{k_\rho}{\xi_1}e^{-\xi_1|z-h|}\right)J_0\left(k_\rho\rho\right)\mathrm{d}k_\rho. \tag{4b}$$

In expressions (4a) and (4b), P and Q are undetermined coefficients that are determined by the boundary conditions, and J_0 is the zero-order Bessel function of the first kind. Here some variables are given by $\rho^2 = x^2 + y^2$, ${k_\rho}^2 = {k_x}^2 + {k_y}^2$, ${\xi_0}^2 = {k_\rho}^2 - {k_0}^2$, and ${\xi_1}^2 = {k_\rho}^2 - {k_1}^2$, where k_0 and k_1 are, respectively, the wave numbers of the air and the ground.

The normal components of the magnetic flux densities and the tangential components of the electric field intensities in two media are continuous at the interface. From the boundary conditions [2], the relationship between G_0 and G_1 is obtained as the following equations:

$$\lim_{z\to 0+}G_0 = \lim_{z\to 0-}G_1, \tag{5a}$$

$$\lim_{z\to 0+}\frac{1}{{k_0}^2}\frac{\partial G_0}{\partial z} = \lim_{z\to 0-}\frac{1}{{k_1}^2}\frac{\partial G_1}{\partial z}. \tag{5b}$$

Substitute (4a) and (4b) into (5a) and (5b); the coefficients P and Q can be obtained and they are shown in the following equations:

$$P = \frac{2{k_0}^2\xi_0}{{k_0}^2\xi_1 + {k_1}^2\xi_0} e^{(\xi_0-\xi_1)h}, \tag{6a}$$

$$Q = \frac{2{k_0}^2\xi_1}{{k_0}^2\xi_1 + {k_1}^2\xi_0} - 1. \tag{6b}$$

So far, we can write the expressions of G_0 and G_1 as (7a) and (7b)

$$G_0(\mathbf{r}) = \frac{1}{4\pi} I_0, \tag{7a}$$

$$G_1(\mathbf{r}) = \frac{1}{4\pi}\left(\frac{e^{-ik_1R}}{R} - \frac{e^{-ik_1R_i}}{R_i} + I_1\right), \tag{7b}$$

$$I_0 = \int_0^\infty \frac{2{k_0}^2 k_\rho}{{k_0}^2\xi_1 + {k_1}^2\xi_0} e^{-\xi_0 z - \xi_1 h} J_0\left(k_\rho\rho\right) dk_\rho, \tag{8a}$$

$$I_1 = \int_0^\infty \frac{2{k_0}^2 k_\rho}{{k_0}^2\xi_1 + {k_1}^2\xi_0} e^{\xi_1(z-h)} J_0\left(k_\rho\rho\right) dk_\rho, \tag{8b}$$

where $R = \sqrt{\rho^2 + (z+h)^2}$ and $R_i = \sqrt{\rho^2 + (z-h)^2}$.

The formulas of Green's function are obtained, but the equations can not be solved directly. The difficulties like oscillations will appear in solving this kind of equations because of the Sommerfeld integrals [18]. To avoid the trouble in computation, a quasistatic situation can be considered under the condition of ELF or SLF. In this case, Wait [19] has shown that ${k_0}^2\xi_1 + {k_1}^2\xi_0 \approx {k_1}^2\xi_0$, $\xi_0 = \sqrt{{k_\rho}^2 - {k_0}^2} \approx k_\rho$, and this approximation has verified available by many scholars, such as Cooray [20].

So we can get the following approximate expression:

$$\begin{aligned} I_1 &\approx \int_0^\infty \frac{2{k_0}^2 k_\rho}{{k_1}^2\xi_0} e^{\xi_1(z-h)} J_0\left(k_\rho\rho\right) dk_\rho \\ &\approx \frac{2{k_0}^2}{{k_1}^2} \int_0^\infty e^{\xi_1(z-h)} J_0\left(k_\rho\rho\right) dk_\rho. \end{aligned} \tag{9}$$

Here use the approximation that Bannister and Dube [4] have verified as $e^{\xi_1(z-h)} \approx e^{ik_1m(z-h)} e^{k_\rho n(z-h)}$, where the constants m and n get values variable for different cases. When $\sqrt{\rho^2 + (z-h)^2} \ll \delta$ (δ is the skin depth), $m = 0$ and $n = 1$. And $\sqrt{\rho^2 + (z-h)^2}$ and δ are of the same order of magnitude, with $m = 0.4$ and $n = 0.96$ for $\sqrt{\rho^2 + (z-h)^2}/\delta < 1$ while $m = 0.96$ and $n = 0.4$ for $1 < \sqrt{\rho^2 + (z-h)^2}/\delta < 10$. This approximation has a good match presented in the paper written by Gavriloska et al. [21].

Thus I_1 is further approximated to the following expression:

$$\begin{aligned} I_1 &\approx \frac{2{k_0}^2}{{k_1}^2} e^{ik_1m(z-h)} \int_0^\infty e^{k_\rho n(z-h)} J_0\left(k_\rho\rho\right) dk_\rho \\ &= \frac{2{k_0}^2}{{k_1}^2} e^{ik_1m(z-h)} \int_0^\infty \frac{e^{k_\rho n(z-h)}}{k_\rho} J_0\left(k_\rho\rho\right) k_\rho dk_\rho. \end{aligned} \tag{10}$$

Use the Sommerfeld identity as follows [22]:

$$\int_0^\infty \frac{e^{-\xi(z-h)}}{\xi} J_0\left(k_\rho\rho\right) k_\rho dk_\rho = \frac{e^{-ikR}}{R}. \tag{11}$$

The expression of I_1 is obtained as

$$\begin{aligned} I_1 &\approx \frac{2{k_0}^2}{{k_1}^2} e^{-ik_1m(-z+h)} \frac{e^{-i\sqrt{{k_\rho}^2 - {k_\rho}^2}\sqrt{\rho^2 + [n(-z+h)]^2}}}{\sqrt{\rho^2 + [n(-z+h)]^2}} \\ &= \frac{2{k_0}^2}{{k_1}^2} \frac{e^{-ik_1m(-z+h)}}{\sqrt{\rho^2 + [n(-z+h)]^2}}. \end{aligned} \tag{12}$$

So far we have got the formula of the underground vector potential as follows:

$$\begin{aligned} \mathbf{A}(\mathbf{r}) = \frac{\mu_1}{4\pi} \int_V \Bigg(&\frac{e^{-ik_1R}}{R} - \frac{e^{-ik_1R_i}}{R_i} \\ &+ \frac{2{k_0}^2}{{k_1}^2} \frac{e^{-ik_1m(-z+h)}}{\sqrt{\rho^2 + [n(-z+h)]^2}} \Bigg) \mathbf{J}\left(\mathbf{r}'\right) dV'. \end{aligned} \tag{13}$$

To solve the current distribution on the antenna surface is the key work of the whole subject. From Maxwell's equations, the relationship expression between the electric field $\mathbf{E}$ and the vector potential $\mathbf{A}$ is shown in

$$\mathbf{E} = -i\omega\mathbf{A} + \frac{1}{\mu\sigma + i\omega\mu\varepsilon} \nabla\nabla \cdot \mathbf{A}. \tag{14}$$

Assuming that there is only vertical current along the z direction on the vertical wire antenna, thus we can make $\mathbf{A} = A_z\mathbf{e}_z$. Taking the fact that the field point coordinates and the source point coordinates are, respectively, (x, y, z) and (x', y', z'), the z component of the electric field can be obtained. Consider the current is distributed on the antenna surface; the axial component of the electric field excited by current is $\mathbf{E}_z$ while the axial component of the electric field excited by other sources is $\mathbf{E}^i{}_z$. Because the antenna surface is considered to be an ideal conductor, by using the boundary conditions of the ideal conductor, the following equation (15) should be satisfied:

$$\mathbf{E}_z(\mathbf{s}) + \mathbf{E}^i{}_z(\mathbf{s}) = 0. \tag{15}$$

When the antenna radius a and the wavelength λ meet the condition $a \ll \lambda$, the assumption that current is uniformly

distributed along the surface is established. Then the effect of the current along the antenna surface is equivalent to a line current along z-axis. Combined with (14), the following expression is obtained:

$$E_z^{\,i} = -\frac{1}{4\pi(\sigma_1 + i\omega\varepsilon_1)}\left(\frac{\partial^2}{\partial z^2} + k_1^{\,2}\right) \cdot \int_{-l}^{0} I(z')\left(\frac{e^{-ik_1R}}{R} - \frac{e^{-ik_1R_i}}{R_i} + \frac{2k_0^{\,2}}{k_1^{\,2}}\frac{e^{ik_1m(z+z')}}{\sqrt{a^2 + [n(z+z')]^2}}\right)dz', \tag{16}$$

where $R = \sqrt{a^2 + (z - z')^2}$ and $R_i = \sqrt{a^2 + (z + z')^2}$.

The MOM [23] is used to solve the current distribution, and pulse base and point matching method are chosen in this section.

Already knowing the current distribution, the vector potential $\mathbf{A}$ concerned can be calculated by (13). Then the axial and radial components of the electric field can be obtained from the following expressions which are derived from (14):

$$E_z = \frac{1}{\mu\sigma + i\omega\mu\varepsilon}\left(\frac{\partial^2}{\partial z^2} + k^2\right)A, \tag{17a}$$

$$E_\rho = \frac{1}{\mu\sigma + i\omega\mu\varepsilon}\frac{\partial^2 A}{\partial\rho\partial z}. \tag{17b}$$

Finally, what we are concerned about is the voltage received by the wire antenna on the ground, and it can be obtained by the following formula about E_ρ:

$$V_r = \sum_i^N \frac{E_\rho(\rho_i) + E_\rho(\rho_{i+1})}{2}(\rho_{i+1} - \rho_i), \tag{18}$$

where V_r is the voltage received on the ground and ρ_i is the distance of the ith point.

3. Numerical Results and Discussion

3.1. Field of the Antenna. Consider a wire antenna in the ground, the top of which is 500 m away from the ground. Assume that the ground is a homogenous medium and the character is that $\sigma = 0.075$ S/m, $\varepsilon = 20\varepsilon_0 = 1.7708 \times 10^{-10}$ F/m, and $\mu = 4\pi \times 10^{-7}$ H/m. The antenna length is $l = 6$ m, and antenna radius is $a = 0.05$ m, with 1 V δ voltage source excitation added on the center. By the skin depth formula $\delta = \sqrt{1/\pi f\mu\sigma}$, we can obtain the skin depth in this case. The distance between the source point and the field point determined by $\sqrt{a^2 + (z - z')^2}$ is far less than the skin depth, so we choose $m = 0$ and $n = 1$ to solve this current distribution problem. Because the current and field studied are all complex numbers, we take the modulus of the complex numbers as the values of the current and field in the following work.

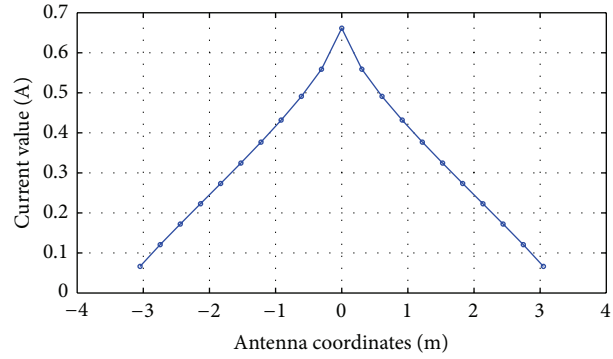

Figure 2: Current distribution on the antenna surface.

The current distribution of the antenna is calculated by MOM; Figure 2 shows the current distribution of the wire antenna in the case of the frequency is 10 Hz. From Figure 2 we can see that the current distribution is approximate triangular distribution, well matching the current distribution of the electrically small antenna.

The following work is to calculate the electric field excited by the antenna. To solve this problem, the value m and n in (13) should be confirmed first. Because the ratio $\sqrt{\rho^2 + (z - h)^2}/\delta$ is between 1 and 10, we take the value $m = 0.96$ and $n = 0.4$.

The changes of the electric field magnitude with the radial distance are shown in Figure 3. The curves of Figure 3(a) show the variation of the axial component of the electric field magnitude with the radial distance on the ground at 10 Hz and 50 Hz, respectively. From that we can see the field magnitude at 50 Hz is higher than that at 10 Hz and both the variation trends are the same with the radial distance. With the increasing radial distance, the magnitude gets smaller and smaller. Curves in Figure 3(b) represent the variation of the radial component of the electric field magnitude with the radial distance on the ground at 10 Hz and 50 Hz, respectively. The trends of the field magnitude with the radial distance both at 10 Hz and 50 Hz are also the same, but the magnitude at 50 Hz is smaller than that at 10 Hz, opposite to the axial component of the electric field magnitude. The radial component of the electric field magnitude becomes larger with the increasing distance first and then becomes smaller after a maximum value. Compared with the radial component of the electric field magnitude, the axial component of the electric field magnitude is several orders smaller, so it only has a slight effect on the total electric field.

The phase of the electric field is shown in Figure 4. The axial component of the electric field phase varies smoothly with the radial distance at different frequencies which is demonstrated in Figure 4(a). The radial component of the electric field phase gradually decreases with the increasing radial distance except that a mutation point appeared near $R = 490$ m at 50 Hz as shown in Figure 4(b).

Figure 5 shows the curves of the variation of the total electric field with the radial distance on the ground, which

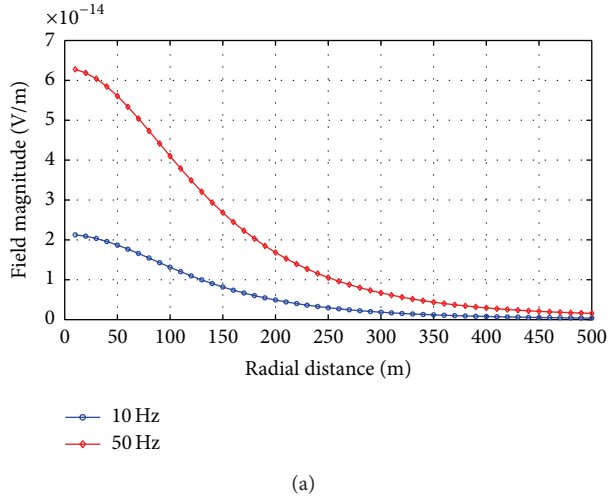

(a)

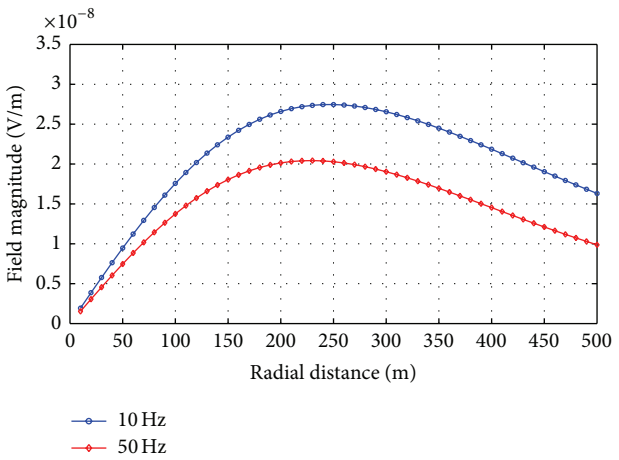

(b)

FIGURE 3: (a) Curves of the axial component of the electric field magnitude; (b) curves of the radial component of the electric field magnitude.

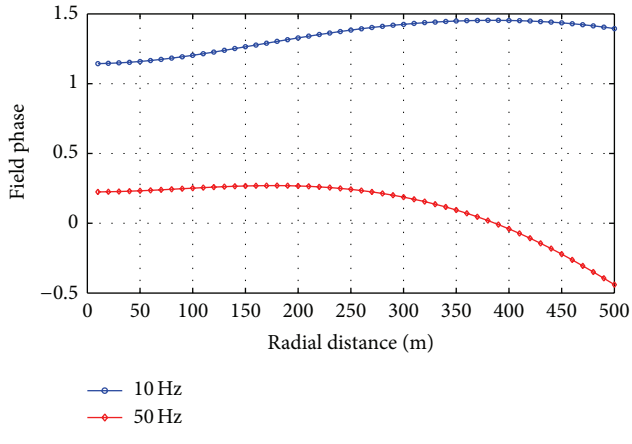

(a)

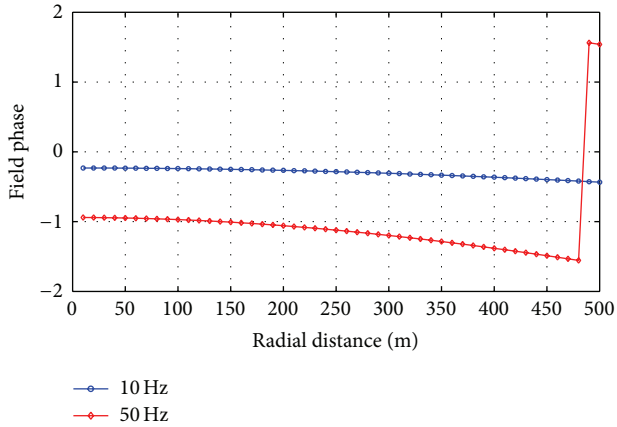

(b)

FIGURE 4: (a) Curves of the axial component of the electric field phase; (b) curves of the radial component of the electric field phase.

look almost the same as those in Figure 3(b). If we make the original point as the relative voltage zero point, the voltage received in radial direction can be calculated. Figure 6 shows the voltage received value on the ground along the radial distance at 10 Hz and 50 Hz, in which the value gets larger when the distance is larger. The voltage received value by the antenna at 50 Hz is smaller than that at 10 Hz.

3.2. Influence of the Frequency and Stratum Parameters. As a further study, the influence of the frequency and stratum parameters on current distribution of the antenna and the electric field generated by the antenna is discussed on the basis of the above study.

The frequency is an important parameter to study first, whose changes can change the value of the current and electric field. In the ELF and SLF band, the maximum value of the current on the antenna surface is chosen to identify the variation with the size of the frequency from 10 Hz to 100 Hz. Figure 7 shows the variation of the maximum current value with the frequency, from which we can see the variation of the current is tiny with a trend that the current value gets smaller with the increasing frequency. In order to know the electric field magnitude variation with the frequency, two points on the ground whose radial distance is 100 m and 200 m are chosen to calculate the concerned radial component of the electric field there. Figure 8 shows the influence of the frequency on the radial component of the electric field magnitude, which tells us that the radial component of the electric field magnitude is negatively correlated with the frequency.

The parameters of the ground can influence the current and electric field as well, one of which is the stratum conductivity. Using the similar method to make the curve of the maximum current value on the antenna surface with the increasing conductivity as shown in Figure 9, we get that the current value has a positive correlation with the conductivity. Curves of Figure 10 demonstrate the variation of the radial component of the electric field magnitude with the conductivity from 0.05 S/m to 0.1 S/m at the two points $R = 100$ m and $R = 200$ m, respectively, where R is the radial distance. With the increasing conductivity, the radial component of the electric field magnitude we concerned about gets smaller at both points either.

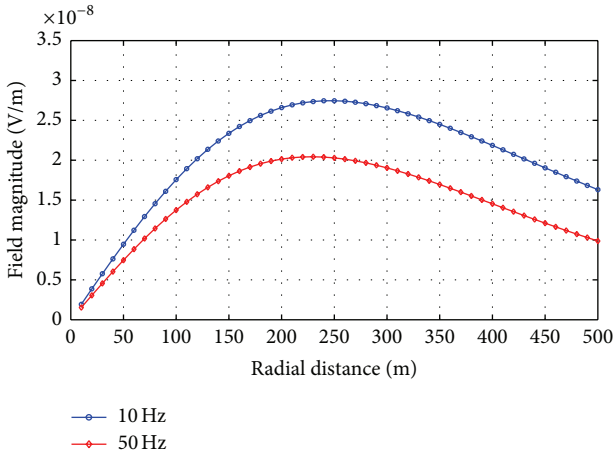

Figure 5: Curves of the total electric field magnitude.

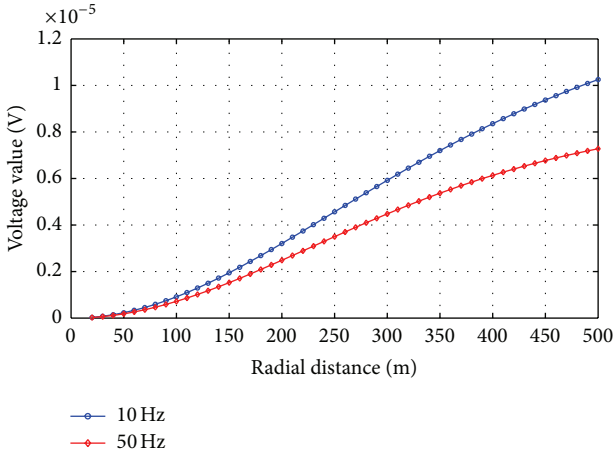

Figure 6: Curves of the received voltage value on the ground.

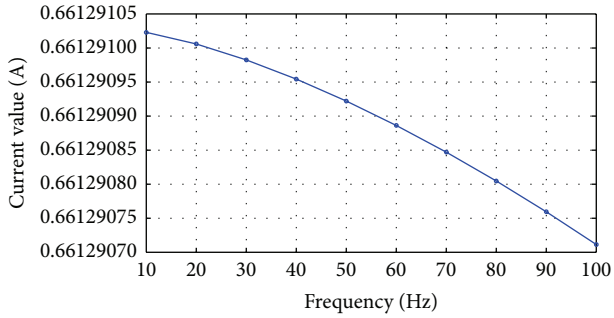

Figure 7: Curve of the maximum current value with the frequency.

Another stratum parameter worth to study is the relative permittivity. Two graphs have made to show the relationship between the field and the relative permittivity. Curve in Figure 11 represents the variation of the maximum current value on antenna surface with the relative permittivity, and the current value gets larger with the increasing relative permittivity. However, the influence of the relative permittivity on current value is so tiny that the current value does not have

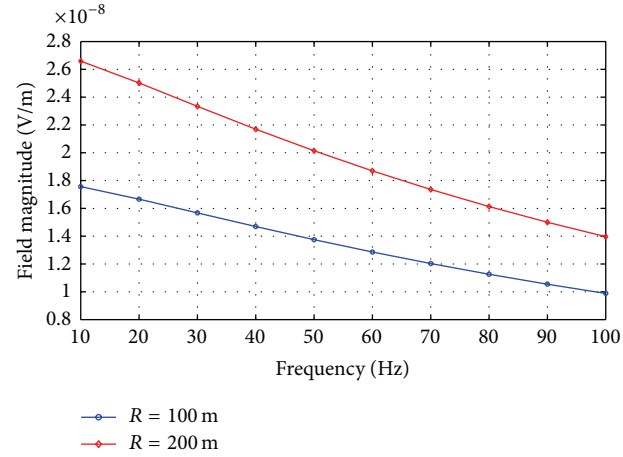

Figure 8: Curves of the radial component of the electric field magnitude with the frequency.

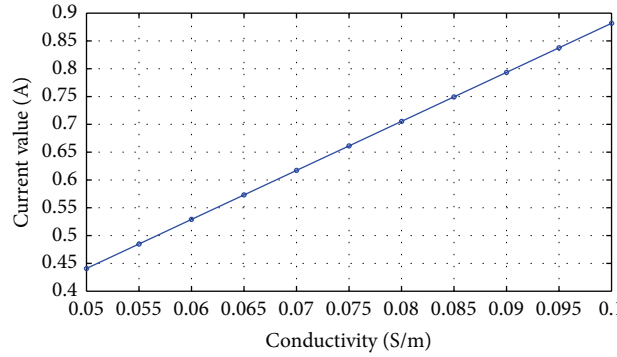

Figure 9: Curve of the maximum current value with the conductivity.

an obvious change. Figure 12 represents the dependence of the radial component of the electric field magnitude with the relative permittivity at the point $R = 200$ m. The magnitude of the radial component of the electric field is negatively correlated with the relative permittivity, and meanwhile the variation is too micro to recognize the difference of the value.

3.3. Verification. As verification, a simulation work has been done using the commercial software HFSS. The model used is the same as the above study with a 10 Hz frequency, and the ground characters are $\sigma = 0.075$ S/m, $\varepsilon = 20\varepsilon_0 = 1.7708 \times 10^{-10}$ F/m, and $\mu = 4\pi \times 10^{-7}$ H/m. The current distribution on the antenna surface is presented in Figure 13. Compared with the results obtained by the mathematical model in Figure 2, the current value near the antenna center of the HFSS results is bigger while the value on both sides of the antenna by HFSS is smaller. Figure 14 shows the variation of the total electric field magnitude along the radial distance, and the maximum magnitude of the field exists at the point $R = 200$ m. The electric field magnitude in this case is a little smaller than the results obtained by the numerical method when the radial distance is farther than 80 m, and the field magnitude is bigger than the corresponding one when

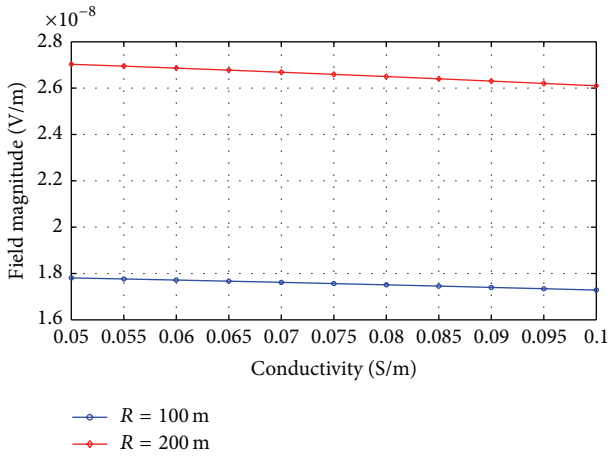

Figure 10: Curves of the radial component of the electric field magnitude with the conductivity.

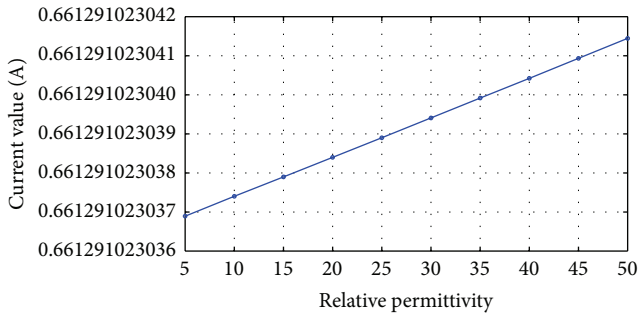

Figure 11: Curve of the maximum current value with the relative permittivity.

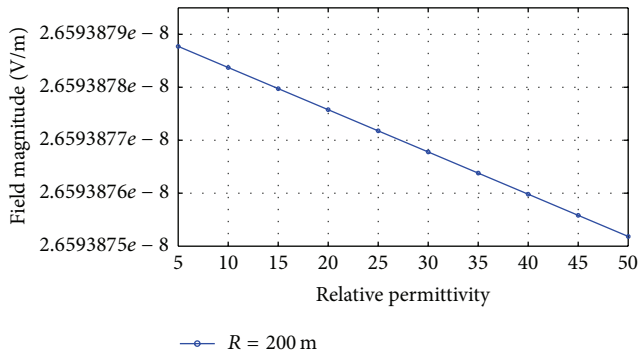

Figure 12: Curves of the radial component of the electric field magnitude with the relative permittivity.

the radial distance is smaller than 80 m. Figure 15 shows the variation of the total electric field phase versus the radial distance, which presents that the field phase by HFSS is a little bigger than the corresponding phase of the numerical results. These differences may be caused by the fact that the model size is too large so that the calculation results by HFSS are not

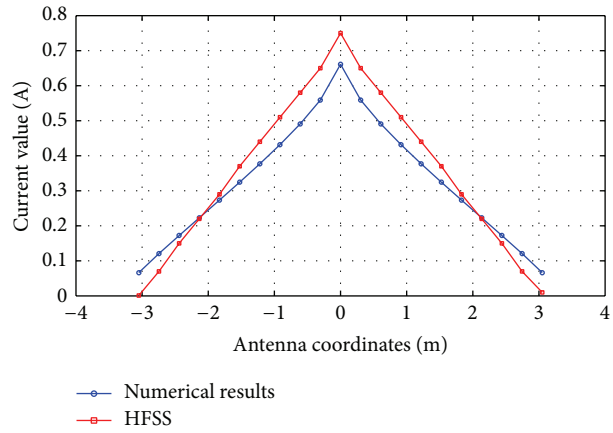

Figure 13: Current distribution on the antenna surface by HFSS.

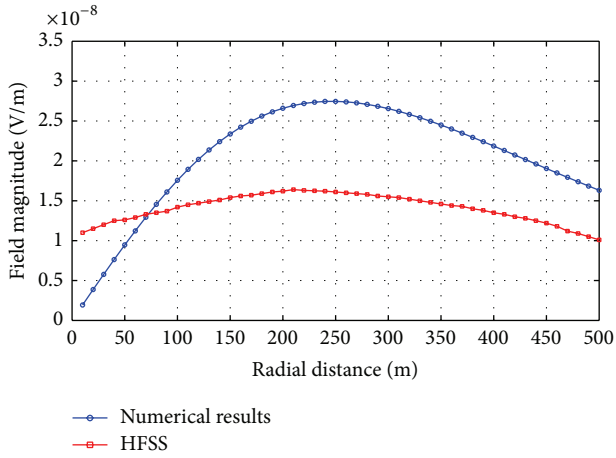

Figure 14: Curve of the total electric field magnitude with the radial distance by numerical results and HFSS.

so accurate, and there are few approximations in the mathematical procedure. As a result, the numerical results are reliable through the verification of the HFSS case, even though there are few differences.

4. Conclusion

An effective model was established to solve the problem of signal transmission through the stratum. In this mathematical model, the expressions of the electric field excited by an underground antenna were derived, which were in forms can be easily solved. Numerical method was used here to obtain the current distribution and the electric field. In these numerical results, the variation of the axial and radial components of the electric field with the radial distance was investigated, and the voltage received on the ground was obtained. From the received voltage signal, we could get the information transferred from underground.

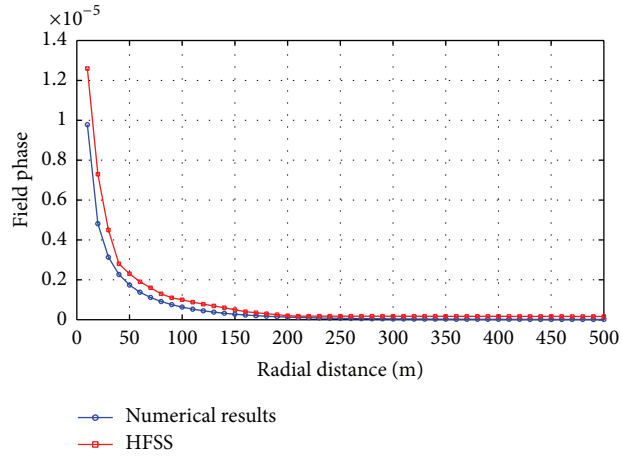

Figure 15: Curve of the total electric field phase with the radial distance by numerical results and HFSS.

The study of the field variation with the frequency and stratum parameters was done and made us know the characters of the antenna underground communications more clearly. Higher frequency will cause larger attenuation on the radial component of the electric field and the total electric field, so SLF and ELF can be the appropriate frequency to apply. The conductivity has a relatively large impact on current and electric field, and the radial component of the electric field magnitude concerned gets smaller when the conductivity gets larger. The relative permittivity only has a slight impact on current and electric field, and there is a negative correlation between the radial component of the electric field magnitude and the relative permittivity.

Conflict of Interests

The authors declare that there is no conflict of interests regarding the publication of this paper.

Acknowledgment

This work is supported by the China Geological Survey Program (no. KZ11Z245).

References

[1] A. Sommerfeld, "Über die Ausbreitung der Wellen in der drahtlosen Telegraphie," *Annalen der Physik*, vol. 386, pp. 1135–1153, 1926.

[2] R. K. Moore and W. E. Blair, "Dipole radiation in a conducting half space," *Journal of Research of the National Bureau of Standards—D*, vol. 65, pp. 547–563, 1961.

[3] P. R. Bannister, *The Image Theory Quasi-Static Fields Of Antennas Above The Earth's Surface*, Defense Technical Information Center (DTIC), 1969.

[4] P. R. Bannister and R. L. Dube, "Simple expressions for horizontal electric dipole quasi-static range subsurface-to-subsurface and subsurface-to-air propagation," *Radio Science*, vol. 13, no. 3, pp. 501–507, 1978.

[5] P. R. Bannister, "Summary of image theory expressions for the quasi-static fields of antennas at or above the earth's surface," *Proceedings of the IEEE*, vol. 67, no. 7, pp. 1001–1008, 1979.

[6] D. C. Chang and J. R. Wait, "Extremely low frequency (ELF) propagation along a horizontal wire located above or buried in the earth," *IEEE Transactions on Communications*, vol. 22, no. 4, pp. 421–427, 1974.

[7] R. W. P. King, "Electromagnetic field of a vertical dipole over an imperfectly conducting half-space," *Radio Science*, vol. 25, no. 2, pp. 149–160, 1990.

[8] R. W. P. King, C. W. Harrison Jr., and V. A. Houdzoumis, "Electromagnetic field in the sea due to an omnidirectional VLF antenna," *Radio Science*, vol. 32, no. 1, pp. 103–112, 1997.

[9] C. T. Tai and R. E. Collin, "Radiation of a Hertzian dipole immersed in a dissipative medium," *IEEE Transactions on Antennas and Propagation*, vol. 48, no. 10, pp. 1501–1506, 2000.

[10] R. Thottappillil, M. A. Uman, and N. Theethayi, "Electric and magnetic fields from a semi-infinite antenna above a conducting plane," *Journal of Electrostatics*, vol. 61, no. 3-4, pp. 209–221, 2004.

[11] A. Khalatpour, R. Sarraf Shirazi, and G. Moradi, "Analysis of vertical wire antennas above lossy half-space using matrix pencil method," *AEU—International Journal of Electronics and Communications*, vol. 64, no. 8, pp. 784–789, 2010.

[12] J. Zou, T. N. Jiang, J. B. Lee, and S. H. Chang, "Fast calculation of the electromagnetic field by a vertical electric dipole over a lossy ground and its application in evaluating the lightning radiation field in the frequency domain," *IEEE Transactions on Electromagnetic Compatibility*, vol. 52, no. 1, pp. 147–154, 2010.

[13] M. P. Rančić and P. D. Rančić, "Horizontal linear antennas above a lossy half-space: a new model for the Sommerfeld's integral kernel," *AEU—International Journal of Electronics and Communications*, vol. 65, no. 10, pp. 879–887, 2011.

[14] D. Poljak, A. Shoory, F. Rachidi, S. Antonijevic, and S. V. Tkachenko, "Time-domain generalized telegrapher's equations for the electromagnetic field coupling to finite length wires above a lossy ground," *IEEE Transactions on Electromagnetic Compatibility*, vol. 54, no. 1, pp. 218–224, 2012.

[15] C. Christakis, K. Ioannidi, S. Sautbekov, P. Frangos, and S. Atanov, "The radiation problem from a vertical short dipole antenna above flat and lossy ground. Novel formulation in the spectral domain with closed form analytical solution in the high frequency regime," http://arxiv.org/abs/1401.1720.

[16] W. Pan and K. Li, *Propagation of SLF/ELF Electromagnetic Waves*, Springer, New York, NY, USA, 2014.

[17] P. DeGauque and R. Grudzinski, "Propagation of electromagnetic waves along a drillstring of finite conductivity," *SPE Drilling Engineering*, vol. 2, no. 2, pp. 127–134, 1987.

[18] G. Fikioris and T. T. Wu, "On the application of numerical methods to Hallen's equation," *IEEE Transactions on Antennas and Propagation*, vol. 49, no. 3, pp. 383–392, 2001.

[19] J. R. Wait, "The electromagnetic fields of a horizontal dipole in the presence of a conducting half-space," *Canadian Journal of Physics*, vol. 39, pp. 1017–1028, 1961.

[20] V. Cooray, "Horizontal electric field above- and underground produced by lightning flashes," *IEEE Transactions on Electromagnetic Compatibility*, vol. 52, no. 4, pp. 936–943, 2010.

[21] O. Gavriloska, M. Mircev, V. Arnautovski, and L. Grcev, "Approximate image formulation for the fields of a horizontal Hertzian dipole in homogenous soil," in *Proceedings of the International PhD-Seminar, Numerical Field Computation and Optimization in Electrical Engineering*, pp. 89–94, 2005.

[22] J. A. Stratton, *Electromagnetic Theory*, vol. 33, John Wiley & Sons, 2007.

[23] R. F. Harrington and J. L. Harrington, *Field Computation by Moment Methods*, Oxford University Press, 1996.